CHEMISTRY
A EUROPEAN JOURNAL

Using Diffusion NMR To Characterize Guanosine Self-Association: Insights into Structure and Mechanism

Mark S. Kaucher,[a] Yui-Fai Lam,[a] Silvia Pieraccini,[b] Giovanni Gottarelli,[b] and Jeffery T. Davis*[a]

Abstract: This paper presents results from a series of pulsed field gradient (PFG) NMR studies on lipophilic guanosine nucleosides that undergo cation-templated assembly in organic solvents. The use of PFG-NMR to measure diffusion coefficients for the different aggregates allowed us to observe the influences of cation, solvent and anion on the self-assembly process. Three case studies are presented. In the first study, diffusion NMR confirmed formation of a hexadecameric G-quadruplex $[G\mathbf{1}]_{16}\cdot 4K^+\cdot 4pic^-$ in CD_3CN. Furthermore, hexadecamer formation from 5′-TBDMS-2′,3′-isopropylidene G**1** and K^+ picrate was shown to be a cooperative process in CD_3CN. In the second study, diffusion NMR studies on 5′-(3,5-bis(methoxy)benzoyl)-2′,3′-isopropylidene G**4** showed that hierarchical self-association of G_8-octamers is controlled by the K^+ cation. Evidence for formation of both discrete G_8-octamers and G_{16}-hexadecamers in CD_2Cl_2 was obtained. The position of this octamer–hexadecamer equilibrium was shown to depend on the K^+ concentration. In the third case, diffusion NMR was used to determine the size of a guanosine self-assembly where NMR signal integration was ambiguous. Thus, both diffusion NMR and ESI-MS show that 5′-*O*-acetyl-2′,3′-*O*-isopropylidene G**7** and Na^+ picrate form a doubly charged octamer $[G\mathbf{7}]_8\cdot 2Na^+\cdot 2pic^-$ **9** in CD_2Cl_2. The anion's role in stabilizing this particular complex is discussed. In all three cases the information gained from the diffusion NMR technique enabled us to better understand the self-assembly processes, especially regarding the roles of cation, anion and solvent.

Keywords: G-quadruplex · NMR spectroscopy · self-assembly · supramolecular chemistry

Introduction

While molecular self-assembly is becoming a powerful approach for nanoscale synthesis,[1] characterization of supramolecules remains a constant challenge. Single crystals of non-covalent assemblies are not always possible. Furthermore, packing forces may give solid-state structures that aren't well-populated in solution. Determination of supramolecular solution structure can also be daunting. Mass spectrometry,[2] analytical ultracentrifugation,[3] dynamic light scattering,[4] gel permeation chromatography and vapor pressure osmometry have been used to determine sizes of supramolecular complexes. None of these techniques, however, provide the atomic resolution offered by NMR spectroscopy. Whereas standard NMR techniques are excellent at determining molecular composition, defining the sizes of high-symmetry complexes can be a problem. For example, NMR spectroscopy cannot readily distinguish a C_4-symmetric tetramer from a C_6-symmetric hexamer, nor can signal integration differentiate an AB dimer and an A_2B_2 tetramer. One method for solving such problems is through the use of pulsed field gradient (PFG) NMR.

PFG-NMR, a method for measuring diffusion rates, provides information about the sizes of molecules in solution.[5] PFG-NMR, used to study self-association of natural products,[6] peptides,[7] and proteins,[8] is also an emerging technique in supramolecular chemistry. Diffusion NMR has been used to define the aggregation state of ion pairs and other organometallic assemblies.[9,10] The sizes of dendrimers, supramolecular polymers and nanoparticles have been determined with the technique.[11–13] Cohen and colleagues have pioneered the use of diffusion NMR in host–guest chemistry, with detailed studies of macrocyclic complexes.[14]

[a] M. S. Kaucher, Dr. Y.-F. Lam, Prof. Dr. J. T. Davis
Department of Chemistry and Biochemistry
University of Maryland, College Park, MD 20742 (USA)
Fax: (+1) 301-314-9121
E-mail: jd140@umail.umd.edu

[b] Dr. S. Pieraccini, Prof. Dr. G. Gottarelli
Dipartimento di Chimica Organica "A Mangini"
Universita di Bologna, Via S. Donato 15
40127 Bologna (Italy)

DOI: 10.1002/chem.200400782

Recently, this technique has been used to investigate issues of structure and mechanism in molecular self-assembly. Hydrogen-bonded rosettes, calixarene–nucleoside conjugates and stacked bisphenylenes have been sized using diffusion NMR,[15–17] and solvation's key role in stabilizing resorcinarene capsules has been revealed.[18] In addition to structural characterization, diffusion NMR can also provide insight into dynamic processes that occur during self-assembly.[19]

We have been actively studying the cation-templated self-assembly of lipophilic guanosine derivatives.[20] Guanosine derivatives organize in the presence of alkali and alkaline earth cations to give hydrogen bonded G-quartets (Scheme 1).[21] These G-quartets undergo further association by stacking into columns known as G-quadruplexes. In addition to serving as models for nucleic acid structures, these lipophilic G-quartets are also the basis for non-covalent synthesis of ionophores, supramolecular polymers, and nanoelectronic devices.[20] A better understanding of assembly–disassembly pathways, including identification of stable intermediates, is critical for learning how to construct and manipulate these synthetic G-quadruplexes. Below, we provide three examples where the use of diffusion NMR to characterize structure also helps illuminate factors that control guanosine self-assembly.

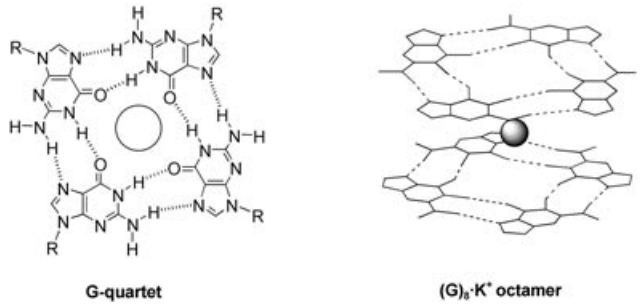

Scheme 1. Cation templated G-quartet structures.

Results

Before describing our results, we discuss some basic information about diffusion NMR.[5] The diffusion rate of a molecule depends on its size and shape, its concentration, the temperature and solvent viscosity. The Stokes–Einstein equation shows that a sphere's diffusion coefficient (D_s) is inversely related to the hydrodynamic radius (R) and solvent viscosity (η), where k is the Boltzmann constant and T is temperature [Eq. (1)].

$$D = \frac{k \cdot T}{6 \cdot \pi \cdot \eta \cdot R} \tag{1}$$

Thus, the ratio of diffusion rates for two different spherical molecules, provided they are in the same environment, is inversely proportional to the ratio of their radii [Eq. (2)].[22,23] Comparative measurements of diffusion rates then help estimate the relative sizes of molecules in solution. This is especially valuable when studying molecular self-assembly, particularly for systems that involve equilibrium formation of different sized complexes.

$$\frac{D_a}{D_b} = \frac{\frac{k \cdot T}{6 \cdot \pi \cdot \eta \cdot R_a}}{\frac{k \cdot T}{6 \cdot \pi \cdot \eta \cdot R_b}} = \frac{R_b}{R_a} \tag{2}$$

Dephasing of an NMR signal, the basis for the diffusion measurements, is influenced by the gradient strength (g), the gradient pulse duration (δ), and the gradient separation time (Δ) between the two opposing gradient pulses.[23,24] Equation (3) shows that the NMR signal intensity is a function of the diffusion coefficient D_s for the case of a rectangular pulse gradient.[5d]

$$I = I_0 \cdot e^{-D \cdot (2\pi \cdot \gamma \cdot g \cdot \delta)^2 \cdot (\Delta - \frac{\delta}{3})} \tag{3}$$

Diffusion coefficients are determined from slopes of normalized signal intensity ($\ln I/I_o$) plotted against the gradient weighting term $(2\pi\gamma g\delta)^2(\Delta-\delta/3)$, where γ is the gyromagnetic ratio of the nucleus being observed. In the standard PFG-NMR pulse sequence, optimized values for the gradient duration (δ) and the gradient separation time (Δ) are kept constant and the gradient strength (g) is varied.[24]

Case 1—Diffusion NMR confirms that G1 forms a hexadecamer in solution: Previously, we showed by X-ray crystallography that 5′-TBDMS-2′,3′-isopropylidene G**1** forms an ordered D_4-symmetric hexadecamer composed of four stacked G-quartets (Scheme 2).[25] This G-quadruplex **2**, with empirical formula $[G\mathbf{1}]_{16}{\cdot}4K^+{\cdot}4pic^-$, is stabilized by four co-axial cations and by four picrate anions. The anions use hydrogen bonds to clamp together the "inner" two G-quartets. Similar solid-state structures for $[G\mathbf{1}]_{16}{\cdot}2M^{2+}{\cdot}4pic^-$ were obtained with the divalent cations Ba^{2+} and Sr^{2+}.[26] Electrospray mass spectrometry of these complexes showed significant amounts of $[G\mathbf{1}]_{16}{\cdot}2M^{2+}$ in the gas phase. Furthermore, NMR mixing experiments in CD_2Cl_2 with $[G\mathbf{1}]_{16}{\cdot}2Ba^{2+}{\cdot}4pic^-$ and $[G\mathbf{1}]_{16}{\cdot}2Sr^{2+}{\cdot}4pic^-$ showed the statistical formation of "homo" and "hetero" complexes, confirming that an intact $[G\mathbf{1}]_{16}$ hexadecamer predominates in solution.[27]

Because of the extensive characterization in the solid, gas, and solution phases, we reasoned that G**1** and its K^+ G-quadruplex **2** would provide an excellent test for using diffusion NMR to characterize guanosine self-association in solution. Our goal was to determine whether we could reliably identify the hexadecamer $[G\mathbf{1}]_{16}{\cdot}4K^+{\cdot}4pic^-$ in an equilibrium mixture that also contained "monomeric" G**1**.[28] Such identification is essential for understanding the factors that control the thermodynamics and kinetics of guanosine self-assembly.

Acetonitrile ($\varepsilon_r = 38.8$) is of suitable polarity to strike a balance between stabilizing the self-assembled hexadecamer **2** and G**1**. For $[G\mathbf{1}]_{16}{\cdot}4K^+{\cdot}4pic^-$ in DMSO ($\varepsilon_r = 45$) no G-

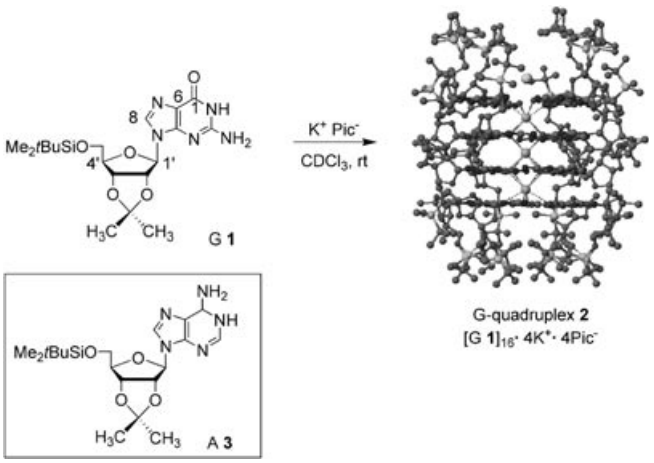

Scheme 2. Structures of G**1**, G-quadruplex $[G\mathbf{1}]_{16}{\cdot}4K^{+}{\cdot}4pic^{-}$ **2** and A**3**.

quadruplex assembly is observed, whereas in the less polar dichloromethane ($\varepsilon_r = 9.1$) only aggregation occurs and no free G**1** is observed. When crystalline $[G\mathbf{1}]_{16}{\cdot}4K^{+}{\cdot}4pic^{-}$ **2** is dissolved in CD_3CN at rt, three sets of ^1H NMR signals are observed (Figure 1). These separate signals, in slow exchange on the NMR chemical shift time-scale, were distinguished using 2D COSY and NOESY experiments.[25] We assigned one set of NMR signals to "monomeric" G**1**, with the understanding that these signals also contained time-averaged contributions from higher oligomers (mostly dimers) that are in fast exchange with monomer.[29] The other two sets of ^1H NMR signals, always present in a 1:1 ratio, arise from the distinct "outer" and "inner" G-quartets that make up the D_4-symmetric $[G\mathbf{1}]_{16}$ hexadecamer **2**.

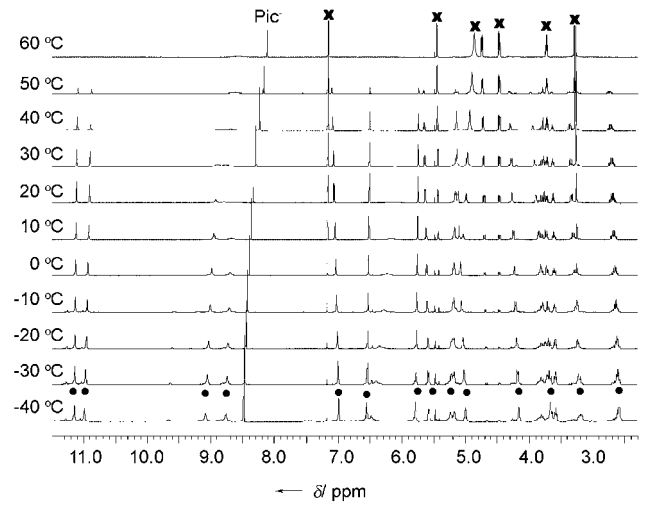

Figure 1. Variable temperature ^1H NMR spectra of $[G\mathbf{1}]_{16}{\cdot}4K^{+}{\cdot}4pic^{-}$ (0.059 mM) dissolved in CD_3CN. Signals for "free" G**1** (×) predominate at higher temperatures, whereas signals for the hexadecameric complex $[G\mathbf{1}]_{16}{\cdot}4K^{+}{\cdot}4pic^{-}$ (●) predominate at lower temperatures.

Diffusion NMR studies were done at 21 °C using a solution prepared by dissolving crystalline $[G\mathbf{1}]_{16}{\cdot}4K^{+}{\cdot}4pic^{-}$ in CD_3CN (0.059 mM), conditions that provide an equilibrium mixture of 94% monomer G**1** and 6% G-quadruplex **2**. The lipophilic adenosine A**3**, which is the same size as G**1** but doesn't self-associate in CD_3CN or interact noticeably with either G**1** or G-quadruplex **2** under these conditions, was used as an internal standard to size the two guanosine species. Before carrying out the diffusion NMR experiments, we calculated an approximate $D_{16mer}/D_{monomer}$ ratio from available crystal structure data. The molecular volume for $[G\mathbf{1}]_{16}{\cdot}4K^{+}{\cdot}4pic^{-}$ is 12140 Å^3 and the molecular volume for G**1** is estimated to be 586 Å^3.[30] Assuming that both molecules are spherical, these volumes provide average hydrodynamic radii of 14.26 Å for $[G\mathbf{1}]_{16}{\cdot}4K^{+}{\cdot}4pic^{-}$ and 5.19 Å for G**1**, values that predict a theoretical $D_{16mer}/D_{G\mathbf{1}}$ ratio of 0.36.[22]

Figure 2 shows the influence of increasing magnetic field gradient strength (g) on the intensity of aromatic signals for the sample containing G**1**, A**3** and G-quadruplex **2**. The corresponding Stejskal–Tanner plots obtained from average values for eight separate diffusion NMR measurements are shown in Figure 2d. Analysis of H8 peak intensities gave diffusion coefficients of $D_s = 13.60 \pm 0.30 \times 10^{-10}\,m^2s^{-1}$ for A**3** (δ 8.21) and $D_s = 12.00 \pm 0.20 \times 10^{-10}\,m^2s^{-1}$ for G**1** (Table 1). The G-quadruplex **2** (δ 6.99 for H8 of the "inner" G-quartet) has a much slower diffusion coefficient in CD_3CN ($D_s = 4.70 \pm 0.10 \times 10^{-10}\,m^2s^{-1}$) than A**3** or G**1**. The experimental diffusion coefficients for G-quadruplex **2** and A**3** (D_s (G**2**)/D_s (A**3**) = 0.35) agree well with the theoretical $D_{16mer}/D_{monomer}$ ratio of 0.36, indicating that hexadecamer $[G\mathbf{1}]16{\cdot}4K^{+}{\cdot}4pic^{-}$ is indeed the structure observed by NMR spectroscopy.

The slower diffusion of G**1**, relative to A**3**, is likely due to significant dimerization of G**1** in CD_3CN.[29] To test this hypothesis, we conducted diffusion NMR experiments on G**1**/A**3** mixtures in [D_6]DMSO, a solvent that completely denatures G-quadruplex **2**. Indeed, G**1** and A**3** have much closer diffusion coefficients in [D_6]DMSO (D_s (G**1**)/D_s (A**3**) = 0.96) than in CD_3CN (D_s (G**1**)/D_s (A**3**) = 0.88), consistent with significant inhibition of G–G dimerization by [D_6]DMSO (Table 1).[31]

Characterization of the hexadecamer $[G\mathbf{1}]_{16}{\cdot}4K^{+}{\cdot}4pic^{-}$ by diffusion NMR confirms an important feature of the cation-templated self-association of G**1**. Namely, hexadecamer **2** is part of an equilibrium with "monomeric" G**1**, and its forma-

Table 1. Diffusion coefficients for G**1** hexadecamer/monomer system.[a]

	D_s (G**1**) ($10^{-10}\,m^2s^{-1}$)	D_s (**2**) ($10^{-10}\,m^2s^{-1}$)	D_s (A**3**) ($10^{-10}\,m^2s^{-1}$)	Ratio D_s (**2**)/D_s (**1**)	Ratio D_s (**2**)/D_s (**3**)	Ratio D_s (**1**)/D_s (**3**)
CD_3CN[b]	12.00 ± 0.20	4.70 ± 0.10	13.60 ± 0.30	0.39	0.35	0.88
[D_6]DMSO[c]	1.90 ± 0.03		1.98 ± 0.03			0.96

[a] The diffusion coefficients are the mean ± standard deviation of eight separate measurements at 21 °C. [b] $[G\mathbf{1}]_{16}{\cdot}4K^{+}{\cdot}4pic^{-}$ **2** and A**3** dissolved in CD_3CN. [c] G**1** and A**3** dissolved in [D_6]DMSO.

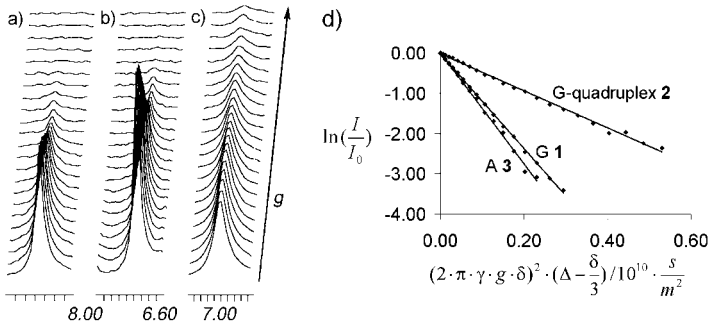

Figure 2. Stack plot of ^{1}H NMR spectra for a mixture of G**1**, G-quadruplex **2** and A**3**. Signals for a) A**3** H8, b) G**1** H8, and c) G-quadruplex **2** "inner" H8 with increasing gradient strength in CD_3CN at 21 °C. d) Stejskal–Tanner plot of G**1**, $[G\mathbf{1}]_{16}{\cdot}4K^+{\cdot}4pic^-$ **2** and A**3** in CD_3CN at 21 °C.

tion is likely to occur via a cooperative nucleation–elongation mechanism.[32] Thus, other than signals for "monomeric" G**1** and hexadecamer **2**, we observe no NMR evidence for any other kinetically stable intermediates in CD_3CN solution. Furthermore, the monomer/hexadecamer ratio in CD_3CN varies significantly with temperature (Figure 1). Thus, at −40 °C, only NMR signals for hexadecamer **2** are observed. As the temperature increases, more G**1** is formed by dissociation from the G-quadruplex. At 60 °C, only G**1** is present. More strong evidence for a cooperative equilibrium was obtained from CD spectroscopy. G-quadruplex **2**, with its stacked G-quartets, has a characteristic CD absorbance centered at 258 nm.[25,33] Figure 3 shows temperature dependent CD data for a solution of $[G\mathbf{1}]_{16}{\cdot}4K^+{\cdot}4pic^-$ in CD_3CN. The sigmoidal melting curve (with $T_m = 25$ °C) is characteristic of a cooperative equilibrium. While more experiments are needed to confirm the nucleation–elongation mechanism,[32] and the presence of positive cooperativity,[34] the NMR and CD data clearly indicate that growth of the [G**1**]16 hexadecamer is coupled to the K^+ templated formation of G-quartets.

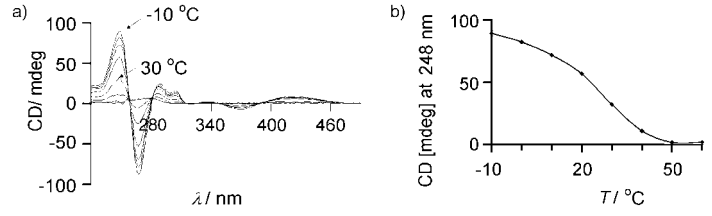

Figure 3. a) Variable temperature CD spectra of $[G\mathbf{1}]_{16}{\cdot}4K^+{\cdot}4pic^-$ **2** in CD_3CN. b) Plot of CD absorbance at 248 nm as a function of temperature.

Case 2—Diffusion NMR shows that hierarchical self-association of G_8-octamers is controlled by the cation: Unlike case 1, where no intermediates were detected in the pathway from monomer to hexadecamer, the next example involves formation of a kinetically stable intermediate. This intermediate, a G_8-K^+ octamer, was readily distinguished from the larger G_{16} hexadecamer with the help of diffusion NMR. The position of the octamer–hexadecamer equilibrium is clearly a function of the K^+ cation concentration in solution (Scheme 3).

Depending on the experimental conditions and the K^+ concentration, NMR spectra indicate that 5′-(3,5-bis(methoxy)benzoyl)-2′,3′-isopropylidene G**4** can form different structures in non-polar solvents CD_2Cl_2 and $CDCl_3$ (Figure 4). Liquid–liquid extraction of K^+DNP^- (DNP: 2,6-dinitrophenolate) (1.2 equiv) from water with G**4** (10 mM) in CD_2Cl_2 provided a single set of ^{1}H NMR signals and a G**4**/DNP ratio of 8:1, consistent with formation of a C_4-symmetric octamer **5** (Scheme 2). However, a different complex was generated when G**4** was used for the solid–liquid extraction of K^+DNP^- (Figure 4b). In the solid-liquid extraction experiment, the two sets of ^{1}H NMR signals in a 1:1 ratio, the 4:1 G**4**/DNP ratio, and the appearance of signals for the hydrogen-bonded N2A amino protons between δ 9.5–9.8 suggested formation of a D_4-symmetric hexadecamer **6** with empirical formula $[G\mathbf{4}]_{16}{\cdot}4K^+{\cdot}4DNP^-$. Since the different complexes, octamer **5** and hexadecamer **6**, exchange slowly on the NMR chemical shift timescale in CD_2Cl_2 (Figure 4c), diffusion NMR was ideal for verifying their relative sizes.

The Stejskal–Tanner plots showing results from diffusion NMR experiments in $CDCl_3$ are shown in Figure 5. Analysis of amide NH peaks at δ 11.74 ppm and at δ 12.28 provided diffusion coefficients of $D_s = 2.45 \pm 0.02 \times 10^{-10}\ m^2 s^{-1}$ for the species with two sets of signals (Figure 4b) and $D_s = 3.13 \pm 0.02 \times 10^{-10}\ m^2 s^{-1}$ for the species with the single set of signals (Figure 4a). This experimental ratio of 0.78 agrees well with the theoretical D_{16mer}/D_{8mer} ratio of 0.79 and supports the proposal that the complex formed by liquid–liquid extraction is octamer **5** with formula $[G\mathbf{4}]_8{\cdot}K^+{\cdot}DNP^-$, whereas the species formed in the solid-liquid extraction is hexadecamer **6**, $[G\mathbf{4}]_{16}{\cdot}4K^+{\cdot}4DNP^-$.

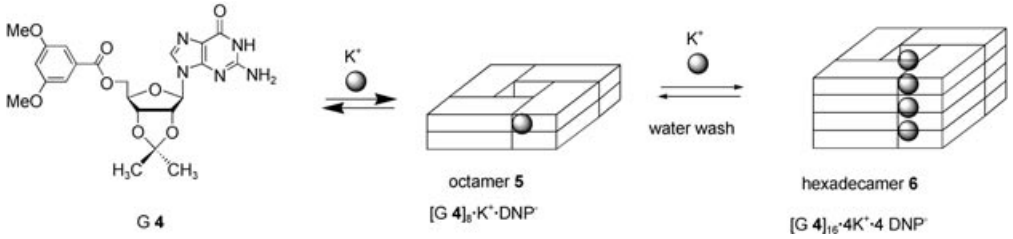

Scheme 3. Formation of $[G\mathbf{4}]_8{\cdot}K^+{\cdot}DNP^-$ **5** and $[G\mathbf{4}]_{16}{\cdot}4K^+{\cdot}4DNP^-$ **6**.

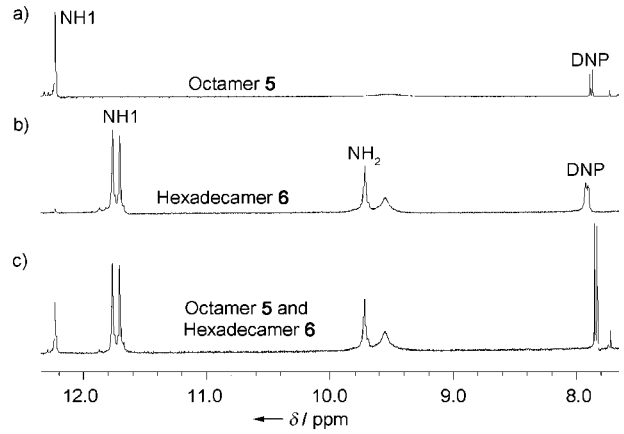

Figure 4. ^{1}H NMR spectra in CD_2Cl_2 at 21 °C of complexes formed by extraction of K(DNP) with G**4**. a) octamer **5**, $[G\mathbf{4}]_8{\cdot}K^+{\cdot}DNP^-$, formed in liquid–liquid extraction; b) hexadecamer **6**, $[G\mathbf{4}]_8{\cdot}K^+{\cdot}(2,6\text{-}DNP)^-$, formed in solid-liquid extraction; c) mixture of octamer **5** and hexadecamer **6**.

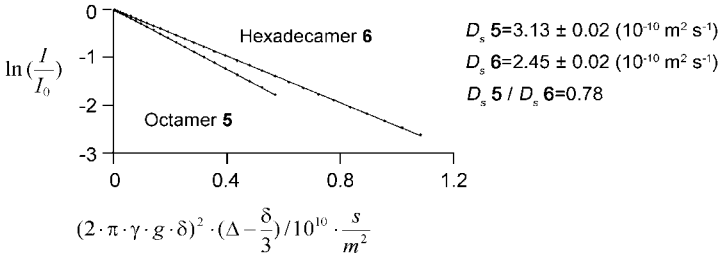

Figure 5. Stejskal–Tanner plot of octamer **5** and hexadecamer **6**. Diffusion coefficients for octamer **5** $[G\mathbf{4}]_8{\cdot}K^+{\cdot}DNP^-$ and hexadecamer **6** $[G\mathbf{4}]_8{\cdot}K^+{\cdot}DNP^-$ in $CDCl_3$ at 21 °C.

The reliable characterization of these different species by diffusion NMR allows us to make firm conclusions about cation-templated self-assembly of G**4** in CD_2Cl_2. First, the C_4-symmetric G_8-octamer **5** is an intermediate in formation of the D_4-symmetric G_{16}-hexadecamer **6**. Second, the K^+ concentration controls this octamer–hexadecamer equilibrium. Under the solid–liquid extraction conditions used to generate $[G\mathbf{4}]_{16}{\cdot}4K^+{\cdot}4DNP^-$ **6**, sufficient K^+ cation is brought into solution to link together two $[G\mathbf{4}]_8{\cdot}K^+$ octamers (Scheme 2). However, this bridging K^+ cation must be held less tightly by hexadecamer **6** than are the cations stabilizing the C_4-symmetric $[G\mathbf{4}]_8{\cdot}K^+$ octamers. This conclusion was supported by an experiment wherein washing a CD_2Cl_2 solution of hexadecamer **6** with water resulted in complete formation of octamer $[G\mathbf{4}]_8{\cdot}K^+{\cdot}DNP^-$ **5**. Likewise, addition of solid K^+DNP^- to a CD_2Cl_2 solution of octamer $[G\mathbf{4}]_8{\cdot}K^+{\cdot}DNP^-$ **5** gave quantitative conversion to hexadecamer **6**. This K^+-dependent switching of the equilibrium between octamer **5** and hexadecamer **6** is similar to NMR solution studies on the human telomere sequence $d(T_2AG_3)$, a G-rich DNA that forms a G-quadruplex monomer at 50 mM K^+ cation concentration and a dimer of co-axial G-quadruplexes at 300 mM K^+ cation concentration.[35]

Case 3—Diffusion NMR reveals size where NMR signal integration is ambiguous: This final example uses diffusion NMR to discriminate between different possible structures with identical component ratios. Solid-liquid extraction of Na^+ picrate into $CDCl_3$ by 5′-*O*-acetyl-2′,3′-*O*-isopropylidene G**7** gave a complex with a single set of NMR signals and a G**7**/picrate molar ratio of 4:1 (Figure 6a). Assuming

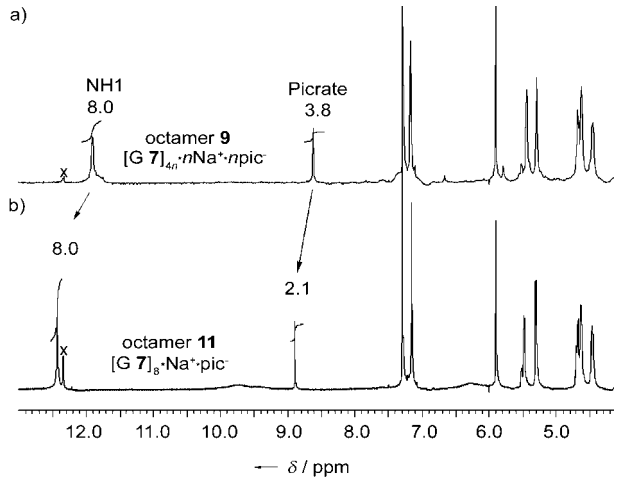

Figure 6. ^{1}H NMR spectra in $CDCl_3$ at 21 °C of complexes formed by extraction of Na picrate with G**7**. a) A species of empirical formula $[G\mathbf{7}]_{4n}{\cdot}n\mathrm{Na}^+{\cdot}n(\mathrm{pic})^-$ formed by solid–liquid extraction; b) octamer $[G\mathbf{7}]_8{\cdot}\mathrm{Na}^+{\cdot}(\mathrm{pic})^-$ **11** formed by washing solution in part a) with water. The identity of the peak with an × is unknown.

one Na^+ cation for each picrate anion, this data indicates formation of a complex with an empirical formula of $[G\mathbf{7}]_{4n}{\cdot}(n)\mathrm{Na}^+{\cdot}n(\mathrm{pic})^-$. As depicted in Scheme 4, the structures that are consistent with this formula are an isolated C_4-symmetric G-quartet, $[G\mathbf{7}]_4{\cdot}Na^+{\cdot}pic^-$ **8**, a pseudo-D_4-symmetric octamer with two bound Na^+ cations, $[G\mathbf{7}]_8{\cdot}2Na^+{\cdot}2pic^-$ **9**,[36] and polymer, $([G\mathbf{7}]_4{\cdot}Na^+{\cdot}pic^-)_n$ **10**. The first two possible structures, a single Na^+-filled G-quartet and a doubly charged octamer, have been previously identified in the gas phase.[37,38] To our knowledge, however, no evidence for either structure in solution has ever been presented.

Polymeric stacks of lipophilic G-derivatives are known to form with the larger K^+ cation, but less is known about the ability of the smaller Na^+ cation to promote formation of polymeric G-quadruplexes.[39]

As shown in Figure 6b, washing the $CDCl_3$ solution of this unknown complex of formula $[G\mathbf{7}]_{4n}{\cdot}(n)\mathrm{Na}^+{\cdot}n(\mathrm{pic})^-$ with water generated a new species. The NMR spectrum was consistent with the D_4-symmetric octamer $[G\mathbf{7}]_8{\cdot}Na^+{\cdot}pic^-$ **11**, namely a single set of peaks, a G**7**/picrate molar ratio of 8:1, and a significant change in only the N1 amide chemical shift ($\Delta\delta = 0.50$ ppm). We suspected that the similar chemical shifts (other than NH1) for $[G\mathbf{7}]_{4n}{\cdot}(n)\mathrm{Na}^+{\cdot}n(\mathrm{pic})^-$ and $[G\mathbf{7}]_8{\cdot}Na^+{\cdot}pic^-$ **11** indicated that $[G\mathbf{7}]_8{\cdot}2Na^+{\cdot}2pic^-$ **9** had

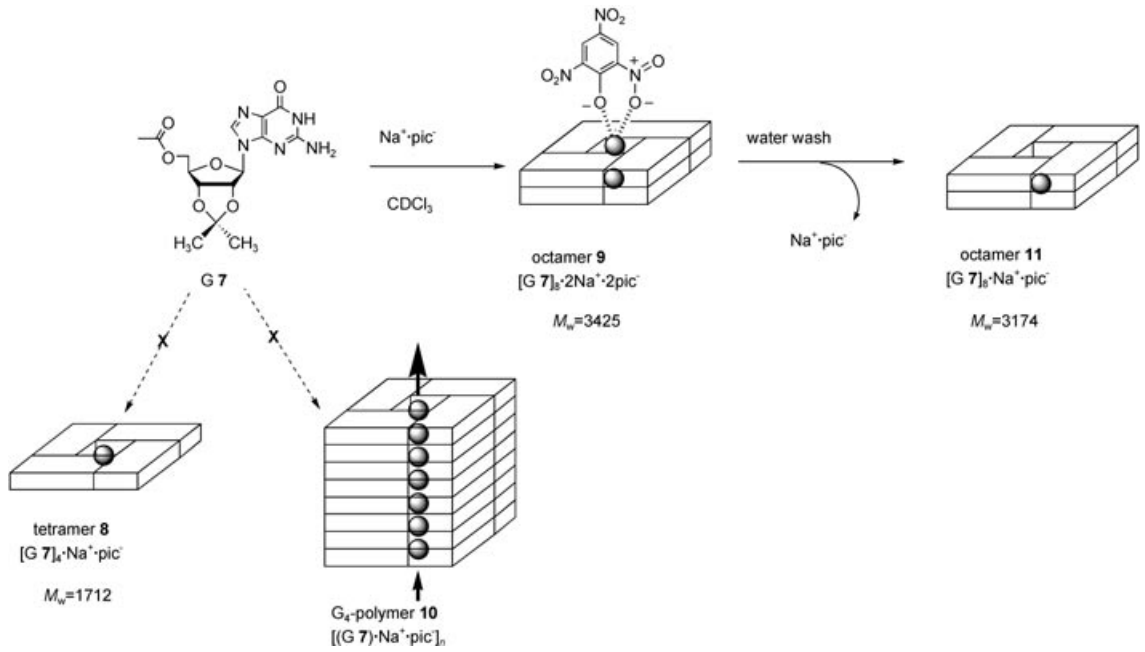

Scheme 4. Self-assembly of G**7** and Na^+ picrate. Tetramer **8**, octamer **9**, and polymer **10** are potential structures for $[G\mathbf{7}]_{4n}\cdot(n)Na^+\cdot n(pic)^-$.

been formed in the solid–liquid extraction of Na^+ picrate, but only diffusion NMR could resolve this structural issue.

As shown in Figure 7, both the octamer $[G\mathbf{7}]_8\cdot Na^+\cdot pic^-$ **11** and the unknown complex generated by solid–liquid extraction, $[G\mathbf{7}]_{4n}\cdot(n)Na^+\cdot n(pic)^-$, had similar CD spectra in

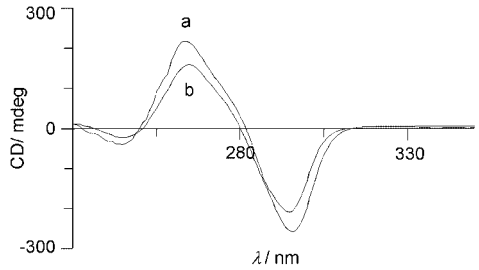

Figure 7. CD spectra of a) complex of formula $[G\mathbf{7}]_{4n}\cdot(n)Na^+\cdot n(pic)^-$ and b) $[G\mathbf{7}]_8\cdot Na^+\cdot pic^-$ **11**. Both samples were at concentrations of 0.43 mM in G**7** in CH_2Cl_2.

CD_2Cl_2, with a degenerate negative exciton couplet centered at 280 nm. This CD signature, corresponding to the long-axis polarized transition of the G chromophore, is diagnostic of an assembly with at least two chiral G-quartets rotated with respect to one another.[33] While this data rules out the isolated G-quartet $[G\mathbf{7}]_4\cdot Na^+\cdot pic^-$ **8** as a structural possibility for $[G\mathbf{7}]_{4n}\cdot(n)Na^+\cdot n(pic)^-$ we could not distinguish octamer $[G\mathbf{7}]_8\cdot 2Na^+\cdot 2pic^-$ **9** and polymeric $([G\mathbf{7}]_4\cdot Na^+\cdot pic^-)_n$ **10** by CD spectroscopy. To solve this problem, we again turned to diffusion NMR measurements.

Because octamer $[G\mathbf{7}]_8\cdot Na^+\cdot pic^-$ **11** and the $[G\mathbf{7}]_{4n}\cdot(n)Na^+\cdot n(pic)^-$ complex were in fast chemical shift exchange in CD_2Cl_2, individual diffusion coefficients for the two different complexes could not be determined from the same NMR experiment (as was done in case 2). Instead, we used A**3** as an internal standard in separate diffusion NMR experiments, with solvent, temperature and concentration held constant. The Stejskal–Tanner plots revealed $D_{exptl}/D_{A\,3}$ values of 0.49 for the octamer $[G\mathbf{7}]_8\cdot Na^+\cdot pic^-$ **11** and 0.47 for the $[G\mathbf{7}]_{4n}\cdot(n)Na^+\cdot n(pic)^-$ complex (Table 2). Both of these experimental diffusion coefficients agree well with the theoretical $D_{8\,mer}/D_{monomer}$ value of 0.50, indicating that the self-assembled species generated by solid–liquid extraction of Na^+ picrate with G**7** must be an octamer bound to two equivalents of Na^+ picrate, namely $[G\mathbf{7}]_8\cdot 2Na^+\cdot 2pic^-$ **9**.

ESI-Mass spectrometry: The diffusion NMR results were bolstered by electrospray mass spectrometry (ESI-MS) of samples sprayed from solutions of $CDCl_3$. Thus, samples generated by the solid–liquid extraction of sodium picrate with G**7** gave the doubly charged octamer $([G\mathbf{7}]_8\cdot 2Na)^{2+}$ (m/z 1484) as the strongest signal in the mass spectrum. A much smaller peak for $([G\mathbf{7}]_{16}\cdot 3Na)^{3+}$ (m/z 1972) was some-

Table 2. Diffusion coefficients for complexes made from G**7**.[a]

	D_s (G**7**) (10^{-10} m^{2}s^{-1})	D_s (Pic) (10^{-10} m^{2}s^{-1})	D_s (A**3**) (10^{-10} m^{2}s^{-1})	Ratio D_s (**7**)/D_s (**3**)	Ratio D_s (Pic)/D_s (**3**)
octamer **9**	4.06 ± 0.10	5.88 ± 0.05	8.62 ± 0.08	0.47	0.68
octamer **11**	4.19 ± 0.05	6.54 ± 0.04	8.60 ± 0.06	0.49	0.76
hexadecamer **12**	3.30 ± 0.07	8.72 ± 0.10		0.38	

[a] The diffusion coefficients are the mean ± standard deviation of eight separate measurements at 21 °C in $CDCl_3$.

times observed at low cone voltages. (40 eV). In contrast, liquid–liquid extraction of sodium picrate with G**7** led to formation of the singly charged ion $([G\mathbf{7}]_8{\cdot}Na)^+$ (m/z 2945) as the major species (Figure 8).[38]

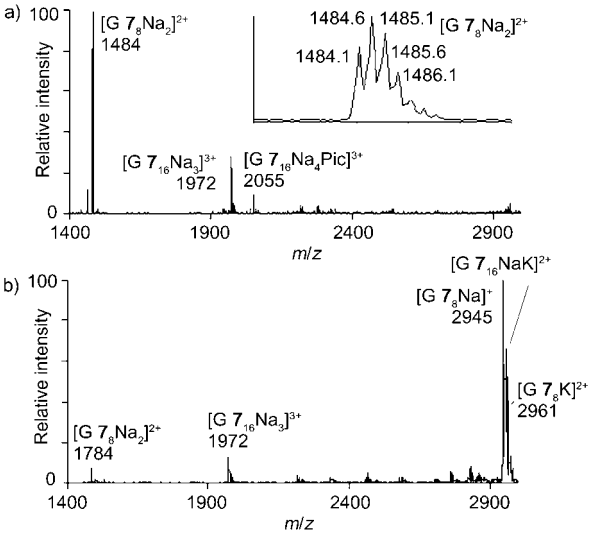

Figure 8. a) ESI-MS spectrum of G**7** in $CHCl_3$ after solid–liquid extraction of Na^+-picrate. b) ESI-MS spectrum of the same solution after washing with water.

We propose that octamer $[G\mathbf{7}]_8{\cdot}2Na^+{\cdot}2pic^-$ **9** is stable under the solid–liquid conditions because the coordination sphere of the "capping" Na^+ in **9** is completed by a picrate anion, thus inhibiting growth of structures such as hexadecamer $[G\mathbf{7}]_{16}{\cdot}4Na^+{\cdot}4pic^-$ under these conditions. The picrate anion is well known to function as a bidendate ligand for metal cations in crown ethers, serving to inhibit formation of sandwich complexes.[40] This proposal is supported by the observation that picrate's NMR signal is shifted far upfield ($\Delta\delta = 0.29$ ppm) in $[G\mathbf{7}]_8{\cdot}2Na^+{\cdot}2pic^-$ **9**, relative to octamer $[G\mathbf{7}]_8{\cdot}Na^+{\cdot}pic^-$ **11**, presumably due to shielding of the bound picrate anion by the nearby G_4-quartet (Figure 6). Similar upfield shifts of the picrate NMR signal, caused by anion–π interactions, have been noted in crown ether chemistry.[40b] Furthermore, the calculated diffusion coefficient for this "capping" picrate in $[G\mathbf{7}]_8{\cdot}2Na^+{\cdot}2pic^-$ **9** ($D_s = 5.88 \pm 0.05 \times 10^{-10}\ m^2 s^{-1}$)[41] is much lower than picrate's diffusion coefficient in $[G\mathbf{7}]_8{\cdot}Na^+{\cdot}pic^-$ **11** ($D_s = 6.54 \pm 0.04 \times 10^{-10}\ m^2 s^{-1}$), also consistent with intimate coordination of this "capping" anion with the guanosine octamer. To test our hypothesis that a "capping" picrate anion stabilizes the octamer $[G\mathbf{7}]_8{\cdot}2Na^+{\cdot}2pic^-$ **9**, we conducted similar solid–liquid extractions in CD_2Cl_2 with $NaPh_4B$, a salt containing the poorly coordinating tetraphenylborate anion. Indeed, the NMR signal pattern (2 sets of signals in a 1:1 ratio) and integration (a G**7**:Ph_4B ratio of 4:1) were consistent with formation of hexadecamer $[G\mathbf{7}]_{16}{\cdot}4Na^+{\cdot}4Ph_4B^-$ **12**.[42] The diffusion coefficient for this complex ($D_s = 3.30 \pm 0.07 \times 10^{-10}\ m^2 s^{-1}$), with A**3** as an internal standard, was also consistent with generation of a hexadecamer ($D_{16mer}/D_{monomer} = 0.38$, see Table 2). These experiments indicate that the counter-anion can dramatically influence the course of guanosine self-assembly.[43]

Conclusion

We presented three examples where the use of diffusion NMR revealed important features about self-assembly of lipophilic guanosines. The confirmation that hexadecamer $[G\mathbf{1}]_{16}{\cdot}4K^+{\cdot}4pic^-$ is stable in CD_3CN solution, in the presence of significant amounts of unassembled G**1**, allowed us to conclude that the cation-templated assembly of G**1** in this polar solvent proceeds via a cooperative equilibrium without formation of significant intermediates. Changing the ligand structure (from G**1** to G**4**) and the solvent (from CD_3CN to CD_2Cl_2) allowed us to identify a discrete octameric intermediate in G-quadruplex formation. Again, the size of this octamer intermediate was confirmed from a series of diffusion NMR experiments. In the last example, diffusion NMR was used to distinguish between possible structures of identical sub-unit stoichiometry. In all three cases the information gained from the diffusion NMR technique enabled us to better understand the self-assembly processes, especially regarding the roles of cation, anion and solvent. We hope to be able to use this structural and mechanistic information to rationally construct and manipulate functional G-quadruplexes.

Experimental Section

All ^{1}H NMR spectra were recorded on a Bruker DRX-400, a Bruker Avance 400 instrument operating at 400.13 MHz, or on a Bruker DRX-500 operating at 500.13 MHz. The ^{13}C NMR spectra were recorded on a Bruker DRX-400 and Bruker Avance 400 instrument operating at 100.61 MHz. Chemical shifts are reported in ppm relative to the residual protonated solvent peak. Variable temperature ^{1}H NMR experiments were controlled to ± 0.1 °C and calibrated with methanol at low temperatures and ethylene glycol at high temperature. Fast atom bombardment (FAB) mass spectra were recorded on a JEOL SX-102A magnetic sector mass spectrometer. Circular dichroism (CD) spectra were recorded on a JASCO-810 spectropolarimeter with a 1 cm path length quartz cuvette. Variable temperature CD experiments were controlled by an attached PFD425S Peltier system with a 1.0 cm path length quartz cuvette. Deuterated solvents were purchased from Cambridge Isotope Laboratories. All chemicals and solvents were purchased from Sigma, Fluka, or Aldrich. Guanosine **1**,[25,44] adenosine **3**,[44] quadruplex **2**,[26] guanosine **7**,[45] and the potassium and sodium phenolates[27] were prepared following published methods.

2′,3′-*O*-Isopropylidene-5′-*O*-(3,5-bis(methoxy)benzoyl)-guanosine (G4): 3,5-Dimethoxy benzoyl chloride (465 mg, 1.5 mmol) was added to a solution of 2′,3′-O-isopropylidene guanosine (500 mg, 1 mmol) and 4-dimethylaminopyridene (5 mg) in distilled pyridine (7.5 mL). The resulting solution was stirred at rt under a N_2 atmosphere for 4 h. The solvent was evaporated under reduced pressure. The remaining white solid was dissolved in CH_2Cl_2 (40 mL) and washed with 0.1 N HCl (10 mL), sat $NaHCO_3$ (10 mL), and H_2O (2 × 10 mL). After removal of the solvent, trituration with Et_2O gave G**4** as a white powder (630 mg, 84%). ^{1}H NMR (400 MHz, [D$_6$]DMSO): δ = 10.84 (s, 1H, NH1), 7.82 (s, 1H, H8), 7.00, (d, 1H, $J = 2.3$ Hz, H8′), 6.76 (t, 1H, $J = 2.3$ Hz, H10′), 6.61

(brs, 2H, NH_2), 6.05 (d, 1H, J=1.5 Hz, H1′), 5.26 (dd, 1H, J=6.0, 1.5 Hz, H2′), 5.24 (dd, 1H, J=6.0, 2.5 Hz, H3′), 4.37–4.51 (m, 2H, H5′), 4.41 (brs, 1H, H4′), 3.77 (brs, 6H, OCH_3), 1.52 (s, 3H, CH_3), 1.32 (s, 3H, CH_3); ^{13}C NMR (100 MHz, [D_6]DMSO): δ = 165.1, 160.5, 156.9, 153.9, 150.4, 136.0, 131.3, 117.0, 113.3, 106.9, 105.2, 88.5, 84.34, 83.9, 81.2, 65.0, 55.5, 27.0, 25.3; HRMS (FAB): m/z: calcd for $C_{22}H_{25}O_8N_5Li$: 494.186, found 494.186 $[M+Li]^+$.

Octamer [G4]$_8$·K$^+$·DNP$^-$ 5: A solution of G**4** (5.0 mg, 10.3 mmol) in CH_2Cl_2 (1 mL) was added to a solution of K$^+$ 2,6-DNP in water (2 mL, 0.65 mM). The resulting biphasic mixture was stirred at rt for 12 h. The organic layer was then separated and concentrated. ^{1}H NMR (400 MHz, CD_2Cl_2): δ = 12.23 (s, 8H, NH1), 7.88 (d, 2H, J=8.1 Hz, mDNP), 7.21 (s, 8H, H8), 7.17 (d, 16H, J=2.3 Hz, H8′), 6.65 (t, 8H, J=2.3 Hz, H10′), 5.90 (s, 8H, H1′), 5.90 (t, 1H, J=8.1 Hz, pDNP), 5.62 (dd, 8H, J=6.3, 2.9 Hz, H3′), 5.24 (d, 8H, J=6.3 Hz, H2′), 4.88 (dd, 8H, J=14.1, 8.5 Hz, H5′$_A$), 4.80–4.74 (m, 16H, H4′, H5′$_B$), 3.80 (s, 48H, OCH_3), 1.68 (s, 24H, CH_3), 1.44 (s, 24H, CH_3).

Hexadecamer [G4]$_{16}$·4K$^+$·4DNP$^-$ 6: A K$^+$ 2,6-DNP solution in water (1 mL, 10.3 mM) was added to a solution of G**4** (5.0 mg, 10.3 mmol) in CH_2Cl_2 (1 mL). The resulting biphasic mixture was stirred at rt for 12 h. The organic layer was then separated and concentrated. The designations a (outer G-quartet) and b (inner G-quartet) in the ^{1}H NMR data refer to the two sets of signals for the hexadecamer. ^{1}H NMR (400 MHz, CD_2Cl_2): δ = 11.76 (s, 8H, NH1a), 11.70 (s, 8H, NH1b), 9.72 (s, 8H, NH_{2A}a), 9.56 (brs, 8H, NH_{2A}b), 7.86 (d, 8H, J=7.6 Hz, mDNP), 7.17 (s, 8H, H8b), 6.97 (s, 8H, H8a), 6.94 (s, 8H, NH_{2B}b), 6.81 (d, 16H, J=2.2 Hz, H8′b), 6.80 (d, 16H, J=2.2 Hz, H8′a), 6.55 (t, 8H, J=2.0 Hz, H10′a), 6.33 (brs, 8H, NH_{2B}a), 6.26 (t, J=2.0 Hz, H10′b), 5.95 (dd, 8H, J=5.9, 3.5 Hz, H2′b), 5.90 (t, 4H, J=7.6 Hz, pDNP), 5.85 (s, 8H, H1′b), 5.74 (dd, 8H, J=6.3, 2.4 Hz, H3′b), 5.53 (d, 8H, J=3.5 Hz, H1′a), 5.33 (brs, 8H, H2′b), 5.23 (d, 8H, J=5.9 Hz, H3′a), 5.04 (t, 8H, J=10.2 Hz, H5′$_A$b), 4.79–4.68 (m, 16H, H4′a, H4′b), 4.54 (dd, 8H, J=11.0, 8.4 Hz, H5′$_A$a), 4.34 (m, 8H, H5′$_B$b), 4.17 (dd, 8H, J=11.0, 4.1 Hz, H5′$_B$a), 3.74 (s, 48H, OCH_3a), 3.38 (s, 48H, OCH_3b), 1.77 (s, 24H, CH_3a), 1.65 (s, 24H, CH_3b), 1.50 (s, 24H, CH_3a), 1.43 (s, 24H, CH_3b).

Octamer [G7]$_8$·2Na$^+$·2pic$^-$ 9: Na$^+$Pic$^-$ (2.0 mg, 8.0 mmol) was added to a solution of G**7** (5.0 mg, 13.7 mmol) in CH_2Cl_2 (1 mL). The resulting suspension was stirred at rt for 12 h. After centrifuging, the organic layer was decanted and concentrated. ^{1}H NMR (400 MHz, $CDCl_3$): δ = 11.86 (s, 4H, NH1), 8.58 (s, 2H, picrate), 7.12 (s, 4H, H8), 5.86 (s, 4H, H1′), 5.39 (dd, 4H, J=5.4, 3.4 Hz, H3′), 5.25 (d, 4H, J=5.4 Hz, H2′), 4.63 (dd, 4H, J=10.8, 5.9 Hz, H5′$_A$), 4.58 (ddd, 4H, J=6.9, 5.9, 3.4 Hz, H4′), 4.41 (dd, 4H, J=10.8, 6.9 Hz, H5′$_B$), 2.23 (s, 12H, Ac), 1.62 (s, 12H, CH_3), 1.42 (s, 12H, CH_3).

Octamer [G7]$_8$·Na$^+$·pic$^-$ 11: A Na$^+$Pic$^-$ solution in water (2 mL, 0.6 mM) was added to a solution of **7** (5.0 mg, 13.7 mmol) in CH_2Cl_2 (1 mL). The biphasic mixture was stirred at rt for 12 h. The organic layer was then separated and concentrated. ^{1}H NMR (400 MHz, $CDCl_3$): δ = 12.38 (s, 8H, NH1), 9.66 (s, 8H, NH_{2A}), 8.85 (s, 2H, picrate), 7.10 (s, 8H, H8), 6.21 (s, 8H, NH_{2B}), 5.85 (s, 8H, H1′), 5.25 (dd, 8H, J=5.9, 3.4 Hz, H3′), 5.25 (d, 8H, J=5.9 Hz, H2′), 4.64 (dd, 8H, J=10.3, 5.9 Hz, H5′$_A$), 4.58 (ddd, 8H, J=6.9, 5.9, 3.4 Hz, H4′), 4.42 (dd, 8H, J=10.3, 6.9 Hz, H5′$_B$), 2.21 (s, 24H, Ac), 1.61 (s, 24H, CH_3), 1.38 (s, 24H, CH_3).

PFG NMR experiments: Diffusion experiments were carried out with a Bruker DRX-500 spectrometer, using the Stimulated Echo Pulse Gradient sequence in FT mode.[46] To improve homogeneity a "13 interval pulse sequence" was used with two pairs of bipolar gradients.[47] All samples for the diffusion measurements were prepared in Shigemi tubes (Shigemi, Inc., Allison Park, PA) and the temperature was actively controlled at 21.0±0.5 °C. Diffusion coefficients were derived using integration of the desired peaks to a single exponential decay, using the "Simfit (Bruker XWINNMR v3.1)" software.

Hexadecamer 2 and adenosine 3 in CD_3CN: Experiments consisted of 24 points with gradient strengths (g) ranging from 0.687–30.91 G cm^{-1}. All experiments comprised 256 scans with a pulse delay of 4 s and δ value of 2.8 ms, Δ value of 99.8 ms, and γ value of 4258 Hz per G. Quadruplex **2** and A**3** were at concentrations of 0.059 and 0.16 mM, respectively.

Guanosine 1 and adenosine 3 in DMSO: Experiments consisted of 24 points with gradient strengths (g) ranging from 0.687–30.91 G cm^{-1}. All experiments comprised 64 scans with a pulse delay of 4 s and δ value of 4.6 ms, Δ value of 199.8 ms, and γ value of 4258 Hz per G. Both G**1** and A**3** were at concentrations of 10.0 mM.

Octamer 5 and hexadecamer 6 in $CDCl_3$: Experiments consisted of 32 points with gradient strengths (g) ranging from 3.420–61.560 G cm^{-1}. All experiments comprised 256 scans with a pulse delay of 4 s and δ value of 2.6 ms, Δ value of 59.9 ms, and γ value of 4258 Hz per G. Octamer **5** and hexadecamer **6** were at concentrations of 0.64 and 0.32 mM, respectively.

Octamer 9, octamer 11 and adenosine 3 in $CDCl_3$: Experiments consisted of 24 points with gradient strengths (g) ranging from 0.687–30.91 G cm^{-1}. All experiments comprised 128 scans with a pulse delay of 4 s and δ value of 2.6 ms, Δ value of 59.8 ms, and γ value of 4258 Hz per G. Octamers (**9** and **11**) and monomer **3** were at concentrations of 1.7 and 6.4 mM, respectively.

Hexadecamer 12 and adenosine 3 in $CDCl_3$: Experiments consisted of 24 points with gradient strengths (g) ranging from 0.687–30.91 G cm^{-1}. All experiments comprised 128 scans with a pulse delay of 4 s and δ value of 2.6 ms, Δ value of 59.8 ms, and γ value of 4258 Hz per G. Hexadecamer **12** and monomer **3** were at concentrations of 0.52 and 4.0 mM, respectively.

ESI-MS experiments: Electrospray mass spectra were recorded with a ZMD Micromass single quadrupole mass spectrometer, operating at m/z 4000. A Hamilton syringe driven by a Harvard pump was used for direct injection of the sample at a rate of 10 μL min^{-1}; a capillary voltage of 3.2 kV and a cone voltage of 40 V were applied, and a desolvation temperature of 120° was used. The charge of the species observed was deduced directly from the spacing of the isotope peaks, a part from the less resolved m/z 2945 signal: the space between the principal peak and the minor adjacent peak at 2961 corresponds to the mass difference between K$^+$ and Na$^+$, indicating a monocharged species. Sample a was prepared by a solid–liquid extraction experiment: a 5 mM chloroform solution of G**7** (2 mL, 0.01 mmol) was stirred over-night in the presence of NaPicrate (4 mg, 16 mmol), and the organic layer was then decanted. Sample b was obtained by washing twice 1 mL of sample a with an equal amount of water: the organic phase was then recovered and injected into the mass spectrometer.

Acknowledgement

This research is sponsored by the Separations and Analysis Program, Division of Chemical Sciences, Office of Basic Energy Sciences, US Department of Energy (J.D.). We are grateful for a NATO Collaborative Grant to J.D. (Maryland) and G.G. (Bologna). We thank Scott Forman and Dr. Mike Shi for their experimental contributions and Prof. Stefano Masiero and Prof. Gian Piero Spada their for helpful comments.

[1] a) G. M. Whitesides, E. E. Simanek, J. P. Mathias, C. T. Seto, D. N. Chin, M. Mammen, D. M. Gordon, *Acc. Chem. Res.* **1995**, *28*, 37–44; b) L. J. Prins, D. N. Reinhoudt, P. Timmerman, *Angew. Chem.* **2001**, *113*, 2446–2492; *Angew. Chem. Int. Ed.* **2001**, *40*, 2382–2426; c) D. N. Reinhoudt, M. Crego-Calama, *Science* **2002**, *295*, 2403–2407.

[2] C. A. Schalley, *Mass Spectrom. Rev.* **2001**, *20*, 253–309.

[3] a) D. Schubert, C. Tziatzios, P. Schuck, U. S. Schubert, *Chem. Eur. J.* **1999**, *5*, 1377–1383; b) L. Isaacs, D. Witt, J. Lagona, *Org. Lett.* **2001**, *3*, 3221–3224; c) J. J. Michels, M. J. O'Connell, P. N. Taylor, J. S. Wilson, F. Cacialli, H. L. Anderson, *Chem. Eur. J.* **2003**, *9*, 6167–6176.

[4] H. Fenniri, B. L. Deng, A. E. Ribbe, *J. Am. Chem. Soc.* **2002**, *124*, 11064–11072.

[5] For some reviews on the technique, see: a) W. S. Price, *New Advances in Analytical Chemistry* (Ed.: E. Atta-ur-Rahman), Gordon and Breach Science, Amsterdam, **2000**, pp. 31–72; b) P. Stilbs, *Prog.*

Nucl. Magn. Reson. Spectrosc. **1987**, *19*, 1–45; c) W. S. Price, *Concepts Magn. Reson.* **1997**, *9*, 299–336; d) W. S. Price, *Concepts Magn. Reson.* **1998**, *10*, 197–237; e) C. S. Johnson, *Prog. Nucl. Magn. Reson. Spectrosc.* **1999**, *34*, 203–256.

[6] a) Ramoplanin: M. C. Lo, J. S. Helm, G. Sarngadharan, I. Pelczer, S. Walker, *J. Am. Chem. Soc.* **2001**, *123*, 8640–8641; b) Okadoic acid: A. H. Daranas, J. J. Fernandez, E. Q. Morales, M. Norte, J. A. Gavin, *J. Med. Chem.* **2004**, *47*, 10–13; c) Progesterone: K. Shikii, S. Sakamoto, H. Seki, H. Utsumi, K. Yamaguchi, *Tetrahedron* **2004**, *60*, 3487–3492.

[7] a) K. H. Mayo, E. Ilyina, H. Park, *Protein Sci.* **1996**, *5*, 1301–1315; b) S. G. Yao, G. J. Howlett, R. S. Norton, *J. Biomol. Nucl. Magn. Reson.* **2000**, *16*, 109–119.

[8] a) P. R. Wills, Y. Georgalis, *J. Phys. Chem.* **1981**, *85*, 3978–3984; b) A. S. Altieri, D. P. Hinton, R. A. Byrd, *J. Am. Chem. Soc.* **1995**, *117*, 7566–7567; c) V. V. Krishnan, *J. Magn. Reson.* **1997**, *124*, 468–473; d) E. Ilyina, V. Roongta, H. Pan, C. Woodward, K. H. Mayo, *Biochemistry* **1997**, *36*, 3383–3388; e) W. S. Price, F. Tsuchiya, Y. Arata, *J. Am. Chem. Soc.* **1999**, *121*, 11503–11512.

[9] For a review: M. Valentini, H. Ruegger, P. S. Pregosin, *Helv. Chim. Acta* **2001**, *84*, 2833–2853.

[10] For some examples: a) S. Beck, A. Geyer, H. H. Brintzinger, *Chem. Commun.* **1999**, 2477–2478; b) I. Keresztes, P. G. Williard, *J. Am. Chem. Soc.* **2000**, *122*, 10228–10229; c) W. H. Otto, M. H. Keefe, K. E. Splan, J. T. Hupp, C. K. Larive, *Inorg. Chem.* **2002**, *41*, 6172–6174; d) E. Martinez-Viviente, P. S. Pregosin, L. Vial, C. Herse, J. Lacour, *Chem. Eur. J.* **2004**, *10*, 2912–2918.

[11] C. B. Gorman, J. C. Smith, M. W. Hager, B. L. Parkhurst, H. Sierzputowska-Gracz, C. A. Haney, *J. Am. Chem. Soc.* **1999**, *121*, 9958–9966.

[12] A. T. ten Cate, P. Y. W. Dankers, H. Kooijman, A. L. Spek, R. P. Sijbesma, E. W. Meijer, *J. Am. Chem. Soc.* **2003**, *125*, 6860–6861.

[13] a) O. Kohlmann, W. E. Steinmetz, X. A. Mao, W. P. Wuelfing, A. C. Templeton, R. W. Murray, C. S. Johnson, *J. Phys. Chem. B* **2001**, *105*, 8801–8809; b) M. Valentini, A. Vaccaro, A. Rehor, A. Napoli, J. A. Hubbell, N. Tirelli, *J. Am. Chem. Soc.* **2004**, *126*, 2142–2147.

[14] a) A. Gafni, Y. Cohen, *J. Org. Chem.* **1997**, *62*, 120–125; b) L. Frish, F. Sansone, A. Casnati, R. Ungaro, Y. Cohen, *J. Org. Chem.* **2000**, *65*, 5026–5030; c) L. Frish, S. E. Matthews, V. Bohmer, Y. Cohen, *J. Chem. Soc. Perkin Trans. 2* **1999**, 669–671; d) L. Frish, M. O. Vysotsky, S. E. Matthews, V. Bohmer, Y. Cohen, *J. Chem. Soc. Perkin Trans. 2* **2002**, 88–93; e) L. Avram, Y. Cohen, *J. Org. Chem.* **2002**, *67*, 2639–2644.

[15] P. Timmerman, J. L. Weidmann, K. A. Jolliffe, L. J. Prins, D. N. Reinhoudt, S. Shinkai, L. Frish, Y. Cohen, *J. Chem. Soc. Perkin Trans. 2* **2000**, 2077–2089.

[16] F. W. Kotch, V. Sidorov, Y. F. Lam, K. J. Kayser, H. Li, M. S. Kaucher, J. T. Davis, *J. Am. Chem. Soc.* **2003**, *125*, 15140–15150.

[17] R. Shenhar, H. Wang, R. E. Hoffman, L. Frish, L. Avram, I. Willner, A. Rajca, M. Rabinovitz, *J. Am. Chem. Soc.* **2002**, *124*, 4685–4692.

[18] a) L. Avram, Y. Cohen, *J. Am. Chem. Soc.* **2002**, *124*, 15148–15149; b) L. Avram, Y. Cohen, *Org. Lett.* **2002**, *4*, 4365–4368; c) L. Avram, Y. Cohen, *Org. Lett.* **2003**, *5*, 1099–1102.

[19] a) C. S. Johnson, *J. Magn. Reson.* **1993**, *102*, 214–218; b) M. F. Lin, C. K. Larive, *Anal. Biochem.* **1995**, *229*, 214–220; c) D. G. Regan, B. E. Chapman, P. W. Kuchel, *Magn. Reson. Chem.* **2002**, *40*, S115–S121; d) E. J. Cabrita, S. Berger, *Magn. Reson. Chem.* **2002**, *40*, S122–S127.

[20] Reviews: a) G. P. Spada, G. Gottarelli, *Synlett* **2004**, 596–602; b) J. T. Davis, *Angew. Chem.* **2004**, *116*, 684–716; *Angew. Chem. Int. Ed.* **2004**, *43*, 668–698.

[21] For original G-quartet references, see: a) M. Gellert, M. N. Lipsett, D. R. Davies, *Proc. Natl. Acad. Sci. USA* **1962**, *48*, 2013–2018; b) T. J. Pinnavaia, H. T. Miles, E. D. Becker, *J. Am. Chem. Soc.* **1975**, *97*, 7198–7200; c) T. J. Pinnavaia, C. L. Marshall, C. M. Mettler, C. I. Fisk, H. T. Miles, E. D. Becker, *J. Am. Chem. Soc.* **1978**, *100*, 3625–3627; for an earlier review, see: d) W. Guschlbauer, J. F. Chantot, D. Thiele, *J. Biomol. Struct. Dyn.* **1990**, *8*, 491–511.

[22] For shapes other than spheres, there are geometric factors that relate diffusion to size: D. C. Teller, E. Swanson, C. DeHaen, in *Methods in Enzymology, Vol. 61* (Eds.: C. H. W. Hirs, S. N. Timasheff), Academic Press, New York, **1979**, pp. 103–124.

[23] E. O. Stejskal, J. E. Tanner, *J. Chem. Phys.* **1965**, *42*, 288–292.

[24] W. S. Price, P. Stilbs, B. Jonsson, O. Soderman, *J. Magn. Reson.* **2001**, *150*, 49–56.

[25] S. L. Forman, J. C. Fettinger, S. Pieraccini, G. Gottarelli, J. T. Davis, *J. Am. Chem. Soc.* **2000**, *122*, 4060–4067.

[26] a) X. D. Shi, J. C. Fettinger, J. T. Davis, *J. Am. Chem. Soc.* **2001**, *123*, 6738–6739; b) X. Shi, J. C. Fettinger, J. T. Davis, *Angew. Chem.* **2001**, *113*, 2909–2913; *Angew. Chem. Int. Ed.* **2001**, *40*, 2827–2831.

[27] X. D. Shi, K. M. Mullaugh, J. C. Fettinger, Y. Jiang, S. A. Hofstadler, J. T. Davis, *J. Am. Chem. Soc.* **2003**, *125*, 10830–10841.

[28] G. Wu, A. Wong, Z. H. Gan, J. T. Davis, *J. Am. Chem. Soc.* **2003**, *125*, 7182–7183.

[29] For references on G–G dimer formation in organic solvents: a) J. Pranata, S. G. Wierschke, W. L. Jorgensen, *J. Am. Chem. Soc.* **1991**, *113*, 2810–2819; b) J. Sartorius, H. J. Schneider, *Chem. Eur. J.* **1996**, *2*, 1446–1452; c) G. Gottarelli, S. Masiero, E. Mezzina, G. P. Spada, P. Mariani, M. Recanatini, *Helv. Chim. Acta* **1998**, *81*, 2078–2092.

[30] The molecular volume for $[G\mathbf{1}]_{16}{\cdot}4K^{+}{\cdot}4pic^{-}$ was taken from its crystal structure as reported in ref. [28]. While we don't have a crystal structure of monomeric G**1**, we have solved the crystal structure of an isomer, 5′-TBDMS-2′,3′-isopropylidene isoguanosine (J. C. Fettinger, V. Sidorov, J. T. Davis, unpublished results). The molecular volume for this isomeric isoG was used as an estimate for the molecular volume of G**1**.

[31] That the D_s (G**1**)/D_s (A**3**) ratio was not unity in [D_6]DMSO is not surprising given that guanosine can form hydrogen-bonded dimers even in this competitive solvent, see: R. A. Newmark, C. R. Cantor, *J. Am. Chem. Soc.* **1968**, *90*, 5010–5017; b) another possible explanation for the decrease in D_s values for G**1**, relative to A**3**, would be chemical exchange of "free" G**1** with the G_{16} hexadecamer during the course of the diffusion NMR experiment. However, 2D-EXSY experiments in CD_3CN at room temperature using a mixing time of $t_m = 99.8$ ms (the same value as the gradient separation time, Δ, in the diffusion NMR experiments) showed no crosspeaks indicative of such monomer-hexadecamer exchange.

[32] a) For a recent review that discusses the differences between cooperative polymerizations that occur under a nucleation-elongation mechanism and non-cooperative, isodesmic polymerations, see: D. H. Zhao, J. S. Moore, *Org. Biomol. Chem.* **2003**, *1*, 3471–3491; b) for an example of the nucleation–elongation mechanism in the formation of hydrogen-bonded, non-covalent polymers, see: V. Simic, L. Bouteiller, M. Jalabert, *J. Am. Chem. Soc.* **2003**, *125*, 13148–13154.

[33] For CD studies on lipophilic G-quadruplexes, see: a) ref. [25] and b) G. Gottarelli, S. Masiero, G. P. Spada, *Enantiomer* **1998**, *3*, 429–436.

[34] For a method to assess cooperativity in self-assembly, see: G. Ercolani, *J. Phys. Chem.* **2003**, *107*, 5052–5057.

[35] Y. Wang, D. J. Patel, *Biochemistry* **1992**, *31*, 8112–8119.

[36] In theory, the doubly charged octamer $[G\mathbf{7}]_8{\cdot}2Na^{+}{\cdot}2pic^{-}$ **9** might be expected to give two sets of NMR signals, but if the "capping" Na^{+} ion is in fast exchange then only a single set of ^{1}H NMR signals would be observed.

[37] K. Fukushima, H. Iwahashi, *Chem. Commun.* **2000**, 895–896.

[38] ESI-MS experiments have identified doubly charged octamers $(G_8{\cdot}2Na)^{2+}$, see: a) I. Manet, L. Francini, S. Masiero, S. Pieraccini, G. P. Spada, G. Gottarelli, *Helv. Chim. Acta* **2001**, *84*, 2096–2107; b) T. Aggerholm, S. C. Nanita, K. J. Koch, R. G. Cooks, *J. Mass Spectrom.* **2003**, *38*, 87–97.

[39] T. Giorgi, F. Grepioni, I. Manet, P. Mariani, S. Masiero, E. Mezzina, S. Pieraccini, L. Saturni, G. P. Spada, G. Gottarelli, *Chem. Eur. J.* **2002**, *8*, 2143–2152.

[40] a) J. Harrowfield, *J. Chem. Soc. Dalton Trans.* **1996**, 3165–3171; b) G. G. Talanova, N. S. A. Elkarim, V. S. Talanov, R. E. Hanes, H. S.

Hwang, R. A. Bartsch, R. D. Rogers, *J. Am. Chem. Soc.* **1999**, *121*, 11281–11290.

[41] The cation's identity is also important. Solid–liquid extraction experiments with G**7** and K^+ picrate gave a mixture of a complex with two sets of signals (presumably hexadecamer) and a complex with one set of signals (presumably octamer). The G-quartet is probably better able to compete with picrate anion for coordinating the larger, more charge-diffuse K^+ ion, thus giving rise to the hexadecamer in this case.

[42] Because of the fast exchange of the two picrate anions in $[G\mathbf{7}]_8{\cdot}2Na^+{\cdot}2pic^-$ **9**, the observed diffusion coefficient represents an average value. In estimating the diffusion coefficient for the "capping" picrate in **9** we assume that the other anion has the diffusion coefficient of the picrate in $[G\mathbf{7}]_8{\cdot}Na^+{\cdot}pic^-$ **11**.

[43] For other examples of an anion influencing the cation-templated formation of G-quadruplexes, see: a) V. Andrisano, G. Gottarelli, S. Masiero, E. H. Heijne, S. Pieraccini, G. P. Spada, *Angew. Chem.* **1999**, *111*, 2543–2344; *Angew. Chem. Int. Ed.* **1999**, *38*, 2386–2388; b) refs. [26b] and [27].

[44] J. T. Davis, S. Tirumala, J. R. Jenssen, E. Radler, D. Fabris, *J. Org. Chem.* **1995**, *60*, 4167–4176.

[45] I. Nowak, M. J. Robins, *Org. Lett.* **2003**, *5*, 3345–3348.

[46] J. E. Tanner, *J. Chem. Phys.* **1970**, *52*, 2523–2526.

[47] R. M. Cotts, M. R. Hoch, T. Sun, J. T. Markert, *J. Magn. Reson.* **1989**, *83*, 252–266; b) Bruker pulse program library, stebpgp 1 s, Avance-version (00/12/13).

Received: July 29, 2004
Published online: November 10, 2004

